



XIX ANIDIS Conference, Seismic Engineering in Italy

## Push ‘o ver: in situ pushover tests on as built and strengthened existing brickwork constructions

Michele Morici<sup>a,\*</sup>, Laura Gioiella<sup>a</sup>, Fabio Micozzi<sup>a</sup>, Alessandro Zona<sup>a</sup>, Allen Dudine<sup>b</sup>, Salvatore Grassia<sup>b</sup>, Carlos Roberto Passerino<sup>b</sup>, Simone Ciotti<sup>c</sup>, Luca Falò<sup>c</sup>, Domenico Liberatore<sup>d</sup>, Luigi Sorrentino<sup>d</sup>, Giacomo Buffarini<sup>e</sup>, Paolo Clemente<sup>e</sup>

<sup>a</sup>Università degli Studi di Camerino, Scuola di Architettura e Design, Viale della Rimembranza 3, 63100 Ascoli Piceno, Italy

<sup>b</sup>Fibre Net S.p.A., Via Jacopo Stellini 3, Z.I.U. 33050 Pavia di Udine, Italy

<sup>c</sup>Di Emidio Progetti Srl, Via Napoleone III 6, 00185 Roma

<sup>d</sup>Sapienza Università di Roma, Dipartimento di Ingegneria Strutturale e Geotecnica, Via Antonio Gramsci 53, 00197 Roma

<sup>e</sup>ENEA, Casaccia Research Centre, via Anguillarese 301, 00123 Roma

---

### Abstract

In the last decades several experimental tests were performed to analyse the seismic capacity of unreinforced masonry, mostly involving small size structural elements or small-scale building models, not accounting for the actual complexity of existing constructions. This paper illustrates experimental pushover tests on two very similar portions of an existing masonry building. The first portion was tested as built, while the second one was tested after a strengthening intervention with Composite Reinforced Mortar (CRM) system with Glass Fiber Reinforced Polymer (GFRP) components. The retrofit consisted in the application of a reinforced plaster on both sides of the walls of the first storey and on the external side only of the second storey, a solution that preserves the continuity of use. Comparisons between the experimental response of the two portions as well as the observed behaviour of the intervention at the first storey (both wall sides) and second storey (only outer side) provide very interesting insights and preliminary information on the degree of upgrading, essential steps to support the assessment of seismic vulnerability reduction.

© 2023 The Authors. Published by Elsevier B.V.

This is an open access article under the CC BY-NC-ND license (<https://creativecommons.org/licenses/by-nc-nd/4.0>)

Peer-review under responsibility of the scientific committee of the XIX ANIDIS Conference, Seismic Engineering in Italy.

*Keywords:* masonry; full-scale pushover test; experimental test; pushing test.

---

\* Corresponding author. Tel.: +39 0737 404287; fax: +39 0737 404272.

E-mail address: [michele.morici@unicam.it](mailto:michele.morici@unicam.it)

## 1. Introduction

Unreinforced masonry buildings are common and widespread traditional structural systems, relying on the availability of affordable materials (blocks and mortar) and the ease of their construction process. However, recent earthquakes (Bam-Iran 2003, L'Aquila-Italy 2009, Elazig-Turkey 2010, Christchurch-New Zealand 2011, Central Italy 2016) highlighted a poor seismic performance of such kind of constructions, especially due to their high structural vulnerability, which leads to significant damages and losses. Even though numerous guidelines were published to assess the performance of existing masonry buildings (ASCE/SEI 41-17 2017, Eurocode 8 2005, NTC2018), the design and modelling tools for these structures still need to be improved. In addition, there is an increasing complexity in the evaluation of their capacities, especially in the case of aggregated masonry structures and in buildings that were subjected to significant changes during their lifetime. More than in other structural materials, experimental techniques are essential tools, widely adopted to understand the behaviour of masonry structures. Among experimental techniques, full-scale testing has a special role and is particularly important when such buildings are retrofitted with innovative solutions where previous experimental evidence could be scarce or null. In the technical literature, some studies (Franklin et al. 2001, Paquette and Bruneau 2003, Beyer 2012a and Beyer and Dazio 2012b, Gattesco et al. 2008, Gattesco et al. 2016) evaluated the response of masonry horizontal spandrels and vertical piers, by investigating in detail the effects of aspect ratio, material type, and boundary conditions. Laboratory tests on small building models were also performed to examine both the stiffness and the strength characteristics of masonry assemblies (Magenes et al. 1995, Magenes and Calvi 1997, Yi 2004, Shahzada et al. 2012, Nicoletti et al. 2020) and these experimental data were used to calibrate numerical models for the design and assessment of masonry structures. Nevertheless, there are only few studies regarding full-scale tests (Aldemir et al. 2015, Aldemir et al. 2018).

In this study full-scale pushing tests performed onto two low-rise very similar portions of an existing building, one in its original condition and the other retrofitted by means of a Fibre Net CRM system with GFRP components (mesh, angles and connectors) and lime - cement based mortar, are presented. A short description of the buildings and of the adopted retrofitting solution is provided together with some information related to the pushing device, the monitoring system, and the sensors used during the tests. Finally, preliminary results are briefly discussed.

## 2. Description of the experimental tests

### 2.1. Geometry of the buildings

The original building, used to derive the two structures investigated (Boccamazzo et al. 2022), is an area hit by the 2016 Central Italy earthquakes. It was built in the first half of the Nineteenth Century, and it was in a bad state of conservation, with diffuse cracking patterns due to the overmentioned seismic events. The building is a two-storey clay-brick masonry structure, with an almost square shape of 11.42 m x 10.87 m, and inter-storey height of 2.80 m (ground floor) and 3.00 m (first floor). Fig. 1a, shows the ground and first storey plans of the original structure, while Fig. 1b shows a picture of the main façade of the building before the interventions and the tests. The masonry structure is made with 2-headed bricks linked by a poor mortar with an overall thickness of 0.25 m. The left part of the first floor of the building is constituted by a jack arch supported by I-beams, while the right side was realized by joists with concrete reinforced precast "I" beams. The roof is built with wood elements, while the shallow foundation is masonry. The plan distributions of the walls, identify two seismic-resistant wall cells separated by a staircase that connects the ground level with the first floor. Once demolished the central staircase and the back annexe, such structural configuration allowed to divide the building into two similar portions, called building 1 and building 2, characterized by the same dimensions and resistance with respect to the horizontal forces (Fig. 1).

The seismic damage suffered by building 1 was repaired by applying standard techniques of interventions (i.e., cracks are repaired with "sew-unsew"), while building 2 was retrofitted by applying a CRM, using mesh, corner elements, preformed composite connectors made of AR glass fibre, thermosetting resins and completed by lime or cement-based structural mortar coatings. The first floor of both the buildings is strengthened with a reinforced concrete (RC) slab connected to the old floor and to the perimetral resisting walls; in this way the horizontal forces are distributed homogeneously among the vertical resisting walls. The wooden roofs are substituted with planar internal steel truss structures, connected to the external masonry walls through RC ring beams working as rigid diaphragms. To restore

the load applied by the roofs to the masonry walls, five boxes filled with water and supported by steel elements are positioned over the RC ring beams. The possible out of plane mechanisms of the walls were blocked by introducing tie rods anchored with external steel slabs at the intermediate and top floors.



Fig. 1. (a) Ground and first floors plant of the building; (b) image of the original building; (c) derived buildings subjected to test.

## 2.2. Tests on materials and components

For the determination of the mechanical parameters of the unreinforced masonry, to correctly design the steel device for the rigid response to the application of the horizontal loads through a couple of high loads hydraulic jacks to the buildings, tests with double flat jacks were made. In this way, compressive strength and elastic modulus of masonry were obtained, together with the compression stress acting in the existing walls at the ground floor. Furthermore, the demolished portion of the building was used for the following in situ tests on walls: tensile tests for bending and compression tests on several brick specimens; single and double flat jack tests to determination of the stress state and of the deformability and strength characteristics of the masonry; diagonal compression tests on non-reinforced masonry. The main results are summarized as follows: the compression tension in masonry was about  $0.29 \text{ N/mm}^2$  at the measure point; the elastic modulus of masonry was  $1278 \text{ N/mm}^2$ ; the tension at the first crack was  $2.0 \text{ N/mm}^2$ ; the diagonal tests provided  $f_{t,RILEM} = 0.228 \text{ N/mm}^2$ ,  $f_{t,0} = 0.152 \text{ N/mm}^2$ ,  $G = 748 \text{ N/mm}^2$ ,  $E = 2135 \text{ N/mm}^2$ . With these values it was possible to calibrate the Fibre Net CRM consolidation system in order not to cause excessive increases in strength and stiffness and evaluate the increase in terms of capacity and deformation of the strengthened building compared to the un-reinforced one. Material tests gave the results reported in Table 1.

Table 1. Identified material parameters.

Element	Compression strength (MPa)	Flexural strength (MPa)	Compression elasticity modulus (GPa)
Structural coating mortar cylinders	11.82	-	9.76
Structural coating mortar prisms	14.55	5.28	-
Cubes of coating (150 mm)	13.44	-	-

### 2.3. Strengthening interventions

The application of the Fibre Net system (Fig. 2) consists in the following steps: 1) Evaluation of the starting phases; 2) Removal of eventual existing plasters; 3) Wetting the to be plastered surface; 4) Initial stretch coat laying; 5) Preparation of the holes for slab-connections; 6) Installation of slab-connections rebars; 7) Preparation of the holes for the connectors; 8) Placement of the mesh and insertion of the connectors; 9) Application of the mortar coating. Using the results obtained from the tests on masonry and on masonry components, the CRM System, applied on both sides of the masonry walls on the Ground Floor and only on external side on the First Floor of the Building 2, was designed thanks to the results of the previous experimental campaigns that permitted to define simple analytical formulas for optimized proportioning.

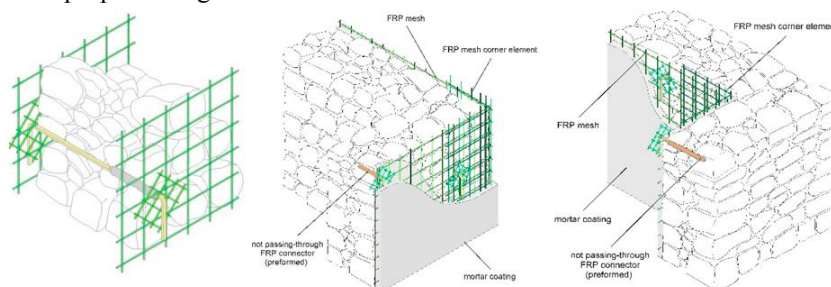


Fig. 2. Fibre Net retrofit intervention system.

Step 1 required the study of the masonry in its initial conditions, in terms of geometry (type of blocks, thickness, presence of different layers, types of joints, etc.) and materials (origin of the blocks, joints of mortars, eventual plaster mortar, eventual presence of diatoms, etc.). Step 2 required the removal of existing plaster and defective parts and subsequently washing the outer layers of masonry using a high-pressure cleaner to obtain a scarification of the joints and removal of the surface portions of disaggregated and non-cohesive mortar. Such action allowed the mortar to penetrate the masonry joints and improve adhesion. Additional actions included washing from top to bottom the façade and re-building the masonry where badly damaged or missing. In step 5 the connection of reinforced mortar to concrete slabs at base or top of the wall was made. Circular section improved adhesiveness rebars in AISI 304 were used, orientated in vertical direction on the surface of the masonry wall to be reinforced. Bar diameters, as well as inter-bar spacing, were determined based on the structural analysis ( $\varnothing 8$  mm) while the recommended bar spacing distance 40 cm was used. In step 8 the mesh was placed on the face intended for inserting the "long" connectors. Afterwards, the stress distributor device was placed on one of the holes provided for the "long" connectors and the connector was inserted by holding stable the device. Then, the mesh was placed on the other side of the wall and resin was injected in the enlarged holes of the holes. A centred stress distribution device was placed on the hole and the connector was inserted by holding the first stable and penetrating the resin previously injected. In step 9 it was necessary to wait for the complete hardening of the connective injection resin before proceeding with the application of the mortar coating. When dust or debris were produced during mesh placement, it was necessary to proceed to the perfect cleaning of the scratched coat before laying the defined mortar coating.

### 2.4. Pushing device

In situ testing requires a strong reaction frame while imposing lateral loads by means of hydraulic actuators. For this purpose, a braced steel frame was built behind the test buildings. The pushing device, similar in concept to the one used in Mazzolani et al. (2004), was made of two portions: a reaction steel frame and a sliding triangular-prism frame, as shown in Fig.2a. Two hydraulic jacks with 5000kN capacity each and equipped with load cells, were adopted to apply the pushing force. A new foundation was built specifically for the test, and it is composed of a concrete slab supported by 8 drilled piles of 800 mm diameter. The pushing device was designed to allow its assembly/disassembly and shifting in the case of other buildings that might be subjected to this same test or other similar. An horizontal

cantilever beam fixed on the edge of the reaction frame supports the triangular frame (as shown in Fig. 3b,c) through a Teflon surface to minimize the friction force during the pushing phase. The ratio between the position of the contact points on the building and the height of hydraulic jacks defines the distribution of the forces applied. In this test the ratio between upper and lower forces is 1.28, to reproduce an inverse triangular pushing profile.



Fig. 3. (a) Pushing system during the test; (b) Assembly of the triangular steel frame; (c) Static scheme of the triangular steel frame.

## 2.5. Monitoring instrumentation

Buildings 1 and 2 were equipped with the same configuration and number of sensors (Fig. 4). Three Linear Displacement Transducers (LDTs) with mechanical stroke of 772 mm (Gefran PC67-750) were installed to monitor horizontal displacements and rotations of the pushing device. One more LDT was positioned behind the triangular prism to evaluate possible differential displacements. The lateral displacements at the story levels were recorded using four LDTs with a lower mechanical stroke of 105 mm (Gefran PZ67-100). Two devices were installed per each floor and per each façade subjected to lateral loads, by means of additional rigid truss structures connected to ground. In this way it was possible to connect the sensors to intermediate concrete floor slab and RC ring beams on the roof. Moreover, the buildings were equipped with eight uniaxial piezoelectric accelerometers used for the dynamic characterization tests. Four high sensitivity PCB 393B31 with 0.5 g peak capacity are applied at the first floor, and four PCB 393A03 with 5 g peak capacity, at the roof level. The overall pushing force was applied through two hydraulic jacks realized by FPT-Fluid Power Technology and controlled by an electric pump with capacity of 700 bar and 1.8 l/m. The level of load transmitted by the pushing device to each building was monitored through two load cells (AEP CLS500t,  $350 \pm 2$  Ohm full bridge based with 5000 kN capacity each).

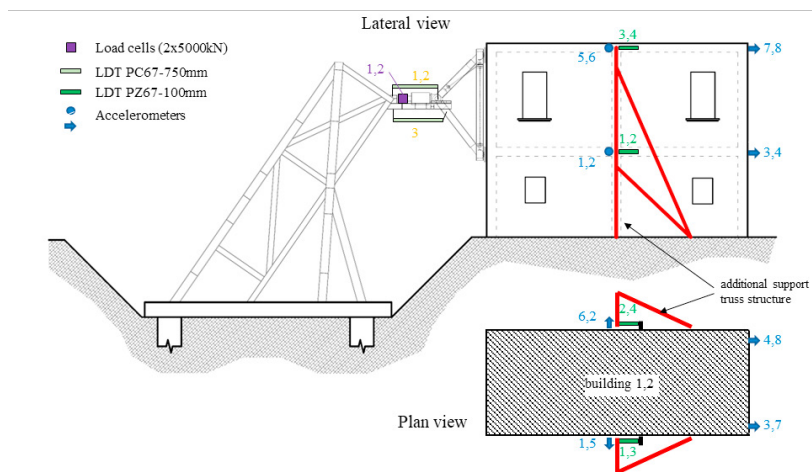


Fig. 4. Sensor layout adopted in the tests for both structures

### 3. Description of the experimental tests

Both structures, i.e., the building as built (building 1) and the retrofitted one (building 2), were subjected to the action of incremental lateral forces, applied to the intermediate and upper floor by means of the pushing device. Such forces are applied into an inverse triangular configuration, representative of a distribution of seismic forces which is proportional to a linear mode shape pushing profile. The pushing phases were organized into different steps and alternated with cycles of full unloading; thus, it is possible to underline stiffness changes of both buildings during the tests. The sub steps of the loading phases were initially determined in terms of force increments,  $\Delta F$ , which better describe the elastic behaviour of the buildings. The used  $\Delta F$  are lower for building 1 (nearly equal to 30 kN each) and higher for building 2, nearly 100 kN. Once the buildings show a change from elastic to inelastic behaviour, namely, when the force becomes nearly the same while the displacements continue to increase, the steps were updated through increments of displacement,  $\Delta u$ , equal to 5 mm per each step. For the sake of brevity and due to space constraints, the results achieved are shown in terms of the enveloped pushover curves, which means without showing the unloading phases. The recorded force is the sum of the forces applied to both the elevations of the buildings, while the displacement is the mean recorded by the LDTs installed at the roof level of the buildings.

#### 3.1. Results for the non-strengthen portion – building 1

Fig. 5a and b report the cracks pattern, which characterizes building 1 at the end of the pushing tests (Fig. 5a) and the related pushover curve (Fig. 5b). The maximum level of force sustained by the building is 396 kN, while the maximum displacement is 53.5 mm. The cracks, underlined by red solid lines in Fig. 5a, are located to both horizontal spandrels and vertical masonry piers. Such cracks highlight the portion of masonry subjected to compression forces, which is mainly the masonry pier located between the openings, but also the sliding due to shear experienced by the concrete beam, located at the roof level. By focusing on the pushover curve, it is possible to observe a quite stiff initial elastic behaviour, up to a lateral force 335 kN with a displacement of nearly 5 mm, while the post-elastic one is characterized by a displacement of 47 mm. The maximum value of the inter-storey drift recorded during the test is close to 1.1% of the storey height, at the upper floor. Such value can be associated to the chord rotation experienced by the vertical pier. It is worth to observe that the Italian Standard NTC 2018 associates the ultimate displacement for a seismic action having a 5% of exceedance probability within 50 years, to a chord rotation that ranges between 0.5% and 1% for masonry piers subjected, respectively to sliding shear and to axial force plus bending moment in its plane. The drift shown by building 1, together with the cracks pattern showed, underlines the coherence of the building performance when subjected to lateral loads, with the code prescription for the safety assessments towards the Collapse prevention Limit State (CLS). The tests were stopped once it was recorded a significant reduction of the force resisted by the building, avoiding possible detachments of masonry.

#### 3.2. Results for the strengthened portion – building 2

Fig. 6a and b refer to the building retrofitted by means of CRM system with GFRP components. It is worth to observe that for this building the openings were farther from the pushing device, with respect to building 1. Nevertheless, also in this case the cracks portrayed in Fig. 6a underline the portion of the masonry subjected to compression, while no sliding due to shear appears at the floor levels (intermediate and roof). Moreover, the cracks are notably thinner and less diffused to the overall façade, if compared to those of building 1. For what concerns the pushover curve, it is worth to observe that the maximum force sustained by the building is 1087 kN, that is 2.74 times that experienced by building 1. Regarding the displacements, instead, the maximum experienced by building 2 is 1.8 times higher than the one of building 1, that is 94.6 mm. Regarding the transition from elastic to anelastic behaviour of building 2, it happens to a force close to 1000 kN and to a displacement of 12.7 mm. This force is nearly 3 times the one that characterizes the end of the elastic behaviour of building 1. For what concerns the inter-storey drift, the maximum value is observed at the first elevation, conversely to what happened for building 1, with a maximum drift equal to 1.8% and a value of 1.3% at the upper floor. The drift values are slightly higher than those expected by the NTC 2018 for masonry piers subjected to bending and axial force due to lateral loads. Nevertheless building 2 was retrofitted to increase its capacity towards lateral loads and these results contribute to testify the effectiveness of the applied retrofitting technique.

Moreover, the ultimate capacity seems to be associated to a ductile mechanism (bending) rather than the sliding shear or the diagonal one, which are brittle failure mechanisms. Fig. 7a and Fig. 7b reports some further detail related to the cracks pattern of the back face of building 2 and to the uplift that the building suffered towards the end of the pushing tests. After retrofitting works, indeed, the dynamic behaviour of the building when subjected to lateral forces became more influenced by a rocking motion, rather than sliding due to shear. The uplift of the building happened nearby the pushing device, where the building was subjected to tension, while the façade opposite to the device is subjected to compression. The tests were stopped when the uplift was nearly equal to 100 mm and the phenomenon involved 2/3 of the length of the building base. It is useful to remember that the buildings are characterized by shallow foundations, on which it was practically impossible to determine and to verify the real effectiveness of the connection.

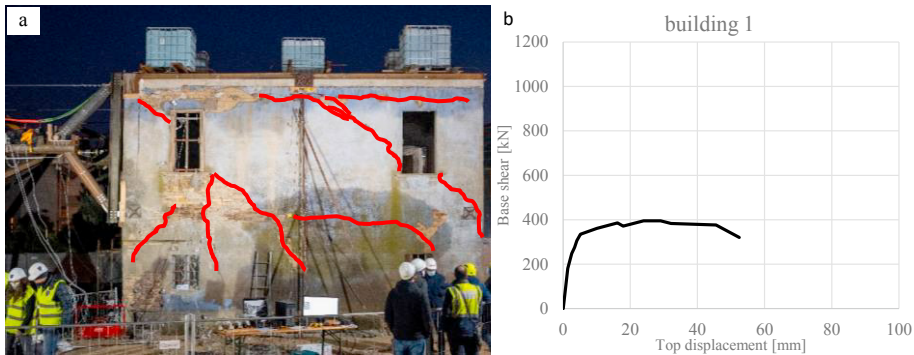


Fig. 5. Building 1: (a) cracks pattern at the end of the test; (b) pushover curve.

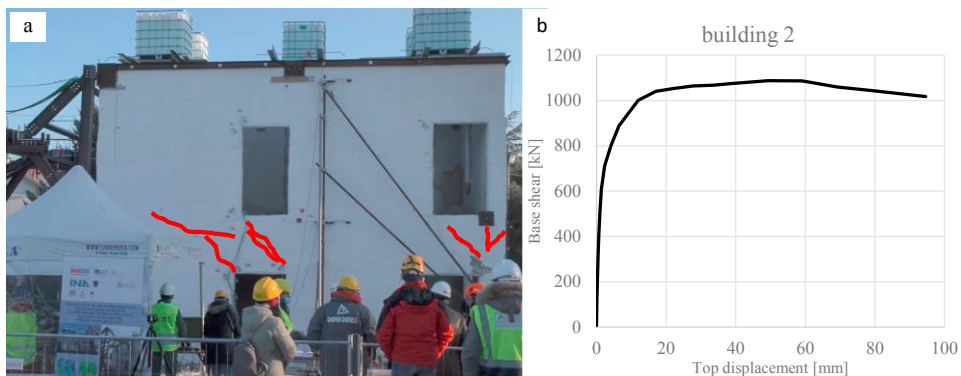


Fig. 6. Building 2: (a) cracks pattern on the front face at the end of the test; (b) pushover curve.

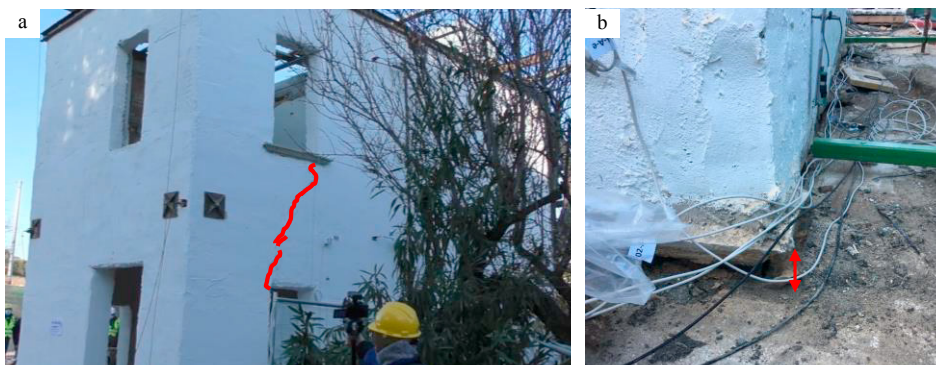


Fig. 7. Building 2: (a) cracks pattern on the back face at the end of the test; (b) uplift of the back left corner.

#### 4. Conclusions

In this study full-scale pushing tests performed on two similar buildings, one as built and the other subjected to retrofitting works by means of Fibre Net CRM system with GFRP components, are presented. Such experimental tests are becoming more and more relevant to shed further light on the ultimate capacity and failure mechanisms of masonry structures, which are usually very vulnerable to earthquakes. Moreover, they also provide the chance to verify and quantify both the efficacy and effectiveness of the applied reinforcement. The preliminary results presented in this work are a first step while more detailed analysis and data processing are being developed.

#### Acknowledgments

The kind contributions to this project by Mr. Franco Emidio Citeroni, Gabriele Gaspari Company, Fibre Net SpA, CMP Srl, and Labortec Ingest Srl are acknowledged.

#### References

- Aldemir, A., Binici, B., Canbay, E., Yakut, A., 2017. Lateral load testing of an existing two story masonry building up to near collapse. *Bulletin of Earthquake Engineering* 15, 3365–3383.
- Aldemir, A., Binici, B., Canbay, E., Yakut, A., 2018. In Situ Lateral Load Testing of a Two-Story Solid Clay Brick Masonry Building. *Journal of Performance of Constructed Facilities* 32, 04018058.
- ASCE/SEI, 41-17 (2017). *Structural Engineering Institute, Structural Engineering Institute, American Society of Civil Engineers (Eds.), 2017. ASCE standard, ASCE/SEI, 41-17: seismic evaluation and retrofit of existing buildings. American Society of Civil Engineers, Reston, Virginia.*
- Beyer, K., 2012. Peak and residual strengths of brick masonry spandrels. *Engineering Structures* 41, 533–547.
- Beyer, K., Dazio, A. 2012. Quasi-static cyclic tests on masonry spandrels. *Earthquake Spectra* 28, 907–929.
- Boccamazzo, A., Di Emidio, G., Diotaiuti G., Dudine A., Dall'Asta A., Micozzi F., Morici M., Liberatore D., Adessi D., Buffarini G., Clemente P., 2022. Push 'o ver: a pushover test program on an existing brickwork construction, Proc. XIX ANIDIS, Turin.
- Franklin, S., J. Lynch, Abrams, D. 2001. Performance of rehabilitated URM shear walls: Flexural behavior of piers. ST6 Project Final Rep. Champaign, IL: Univ. of Illinois at Urbana–Champaign.
- Gattesco, N., Clemente, I., Macorini, L., Noe' S., 2008. Experimental investigation on the behaviour of spandrels in ancient masonry buildings. *Proceeding of 14th World Conference on Earthquake Engineering, October 12-17, 2008, Beijing, China.*
- Gattesco, N., Macorini, L., Dudine, A., 2016. Experimental Response of Brick-Masonry Spandrels under In-Plane Cyclic Loading. *J. Struct. Eng., 10.1061/(ASCE) ST.1943-541X.0001418, 04015146.*
- Magenes, G., Calvi, G.M. 1997. In-plane seismic response of brick masonry walls. *Earthquake Engineering and Structural Dynamics* 26, 1091–1112.
- Magenes, G., Kingsley, G.R., Calvi, G.M. 1995. Seismic testing of a full-scale, two-story masonry building: Test procedure and measured experimental response. *Experimental and Numerical Investigation on a Brick Masonry Building Prototype Rep. No. 3.0. Pavia, Italy.*
- Mazzolani, F.M., Della Corte, G., Faggiano, B. 2004. Seismic upgrading of RC buildings by means of advanced techniques: the ILVA-IDEM project. *13th World Conference on Earthquake Engineering Vancouver, B.C., Canada.*
- Nicoletti, V., Arezzo, D., Carbonari, S., Gara F., 2020. Expeditious methodology for the estimation of infill masonry wall stiffness through in-situ dynamic tests – *Construction and Building Materials*, 262, 120807. Indexed 2020.12.22; published November 30, 2020.
- NTC 2008. *Norme Tecniche per le Costruzioni, 2018 – Ministry of Infrastructures and Transportation, D.M. 17 January 2018. In Italian.*
- Paquette, J., Bruneau, M. 2003. Pseudo-dynamic testing of unreinforced masonry building with flexible diaphragm. *Journal of Structural Engineering* 129, 708–716.
- Shahzada, K., Khan, A.N., Elnashai, A.S., Ashraf, M., Javed, M., Naseer, A., Alam, B. 2012. Experimental seismic performance evaluation of unreinforced brick masonry buildings. *Earthquake Spectra* 28, 1269-1290.
- Yi, T. 2004. Experimental investigation and numerical simulation of an unreinforced masonry structure with flexible diaphragms. Ph.D. dissertation, Dept. of Civil and Environmental Engineering, Georgia Institute of Technology.